

AlGaIn/GaN Schottky Gate Fin-HEMT Fabricated on 8-inch Silicon (111) Substrate with Thin Buffer Layer

Li-Cheng Chang¹, Cheng-Jia Dai¹, Ming Yang¹, Yi-Hong Jiang¹, and Chao-Hsin Wu^{1,2}

¹Graduate Institute of Electronics Engineering, National Taiwan University, Taipei, Taiwan

²Graduate Institute of Photonics and Optoelectronics, National Taiwan University, Taipei, Taiwan

Phone: +886-2-3366-3694 E-mail: chaohsinwu@ntu.edu.tw

Abstract

In this letter, we demonstrate the AlGaIn/GaN Fin-HEMT on 8-inch Si (111) substrate with thin AlGaIn buffer which is about 3 μm . This Fin-HEMT is characterized by the Schottky gate without any insulating dielectric. This Schottky gate creates the depletion region on both sidewalls of the fin channel can further deplete the carrier. This sidewall assistant makes the device turns off earlier than planar device which is confirmed by the positive shift of the threshold voltage (V_{TH}). The minimum fin width is characterized by 100 nm and the corresponding V_{TH} is -0.5 V which has 3.05 V shift from the planar device.

1. Introduction

Owing to the superior material properties such as high breakdown field, low ON-resistance (R_{ON}), and high thermal stability, GaN-based high-electron-mobility transistors (HEMTs) have huge potential of the applications in power electronics [1-3]. In terms of material properties, AlGaIn/GaN heterojunction exhibits 2DEG inherently due to its unique properties of polarization but also results in normally-ON operation. For the normally-ON, i. e., enhancement-mode (E-mode) device, it is more complicated for circuit design and less output efficiency. In this paper, we utilize the fin-shaped channel to modulate the threshold voltage (V_{TH}) toward positive value [4,5]. The gate metal in our Fin-HEMT is deposited directly on the AlGaIn/GaN fin channel to form the Schottky contact on all sides of fin. It should be noted that the Schottky contact has wider depletion width than the metal-insulator-semiconductor contact. Therefore, once the fin becomes narrow enough, it is possible to fully deplete 2DEG through the sidewall depletion region earlier than the top-gate control. This leads to the positive V_{TH} movement and the switching mechanism is similar to the metal-semiconductor field-effect transistor.

2. Device Fabrication

The epitaxial structure of AlGaIn/GaN is grown by MOCVD and starts on 8 inch silicon wafer with a 300 nm AlN nucleation layer, $\sim 3.2 \mu\text{m}$ graded AlGaIn buffer, 2 μm undoped GaN layer, 30 nm undoped $\text{Al}_{0.3}\text{Ga}_{0.7}\text{N}$ barrier, and 1 nm undoped GaN cap layer. The specific layer structure is shown in Fig. 1 (a). After the material growth, hall measurement is implemented form the center to the edge of wafer with 9 points. The results show that peak and average mobility is $1520 \text{ cm}^2/\text{Vs}$ and $1323 \text{ cm}^2/\text{Vs}$, respectively which

suggest that high uniformity of the epitaxy.

The process flow and schematic diagram of device are shown in Fig. 1 (b) and the device is begun with fin formation. The minimum fin width (W_{fin}) here is 100 nm which defined by the electron-beam lithography and is etched by the Cl_2/BCl_3 mixed plasma. The Ti/Al/Ni/Au deposition and rapid thermal annealing is then applied in sequence to form the S/D Ohmic contact. Finally, gate metal with Ni/Au is deposited to complete the device. It should be noted that gate metal is deposited directly on the fin channel to form the Schottky contact on all sides. Fig. 2 is the SEM image of the device with 100 nm W_{fin} . The fin number of 100 nm W_{fin} is 100 and thus we can defined the projective channel width is the production of W_{fin} and fin number.

3. Results and Discussions

The comparison of the transfer characteristics with different W_{fin} is shown in Fig. 3 (a). We can observe that the V_{TH} of the fin device has significant shift toward positive value comparing to planar one. The V_{TH} of device with W_{fin} of 100 nm and gate length (L_g) of 2 μm is characterized by -0.7 V and the planar one is -3.75 V with the same L_g and the gate width (W_g) is 60 μm . The V_{TH} is defined by the current density of 100 $\mu\text{A}/\text{mm}$ normalized by the projective

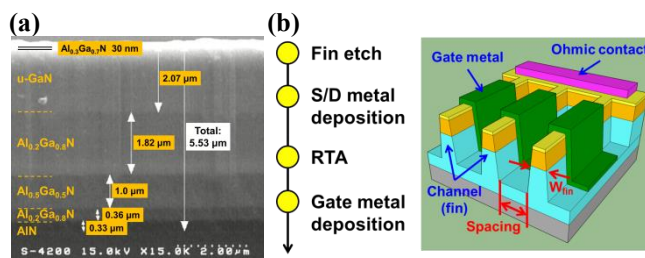


Fig. 1. (a) Layer structure of the 8-inch AlGaIn/GaN-on-Si. (b) Process flow and schematic diagram of our Fin-HEMT. It should be noted that gate metal is deposited directly on the fin channel.

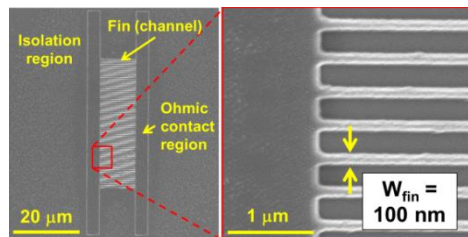


Fig. 2. SEM image of the Fin-HEMT with the minimum W_{fin} of 100 nm.

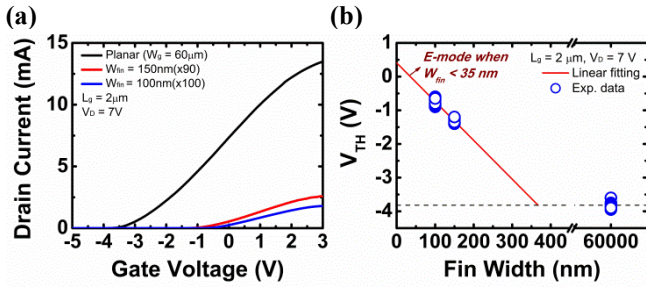


Fig. 3. (a) The comparison of the transfer characteristics with different W_{fin} . (b) The relation between the V_{TH} and the W_{fin} .

channel width. The relation between the V_{TH} and the W_{fin} is also shown in Fig. 3 (b). It can be obtained that while the channel width is in the nano regime, V_{TH} is strongly affected by the W_{fin} . This is attributed to the assistant of depletion region on both sidewalls of fin channel. The switching mechanism of Fin-HEMT is shown in Fig. 4. Once the fin is thin enough, the depletion region caused by the sidewall can fully deplete the 2DEG in channel earlier than the top-gate control. That is, the depletion width on each side is larger than the half of W_{fin} in the specific gate bias and thus results in the pinch-off status. Also, by the linear fitting of V_{TH} with different W_{fin} in Fig. 3 (b) the device with W_{fin} less than 35 nm can obtain the E-mode operation through the side-gate control. And device with the W_{fin} larger than 360 nm, it becomes the top-gate control which is just like the planar one.

The output characteristics of device with 2- μm L_g and 150-nm W_{fin} is shown in Fig. 5 (a). The saturation drain current is 73 mA/mm. This relatively low value is attributed to large source/drain resistance (R_{SD}) of 35.83 $\Omega\text{-mm}$. R_{SD} here is obtained by linear extraction of R_{ON} with different L_g which is shown in Fig. 5 (b). This high R_{SD} is induced by the non-optimized contact resistance and large distance of gate-to-source (L_{gs}) and gate-to-drain (L_{gd}) (both are 5 μm). Therefore, better ON-state performance can be obtained with optimized Ohmic contact and further scaling of the L_{gs} and L_{gd} .

Finally, we compare the ON-state performance of device with different W_{fin} which is shown in Fig. 6. Fig. 6 (a) shows the peak transconductance (g_m) of device with 2 μm L_g . Fin device exhibits higher g_m than the planar one and similar trend of R_{ON} is also obtained in Fig. 6 (b). This is

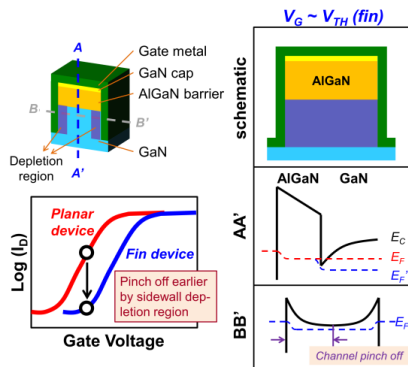


Fig. 4. The switching mechanism of Fin-HEMT.

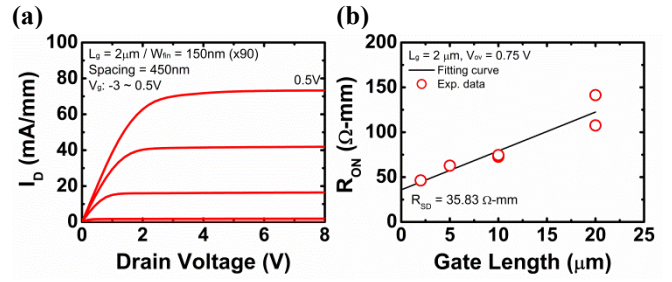


Fig. 5. (a) Output characteristic and (b) R_{SD} extraction of the Fin-HEMT with W_{fin} of 150 nm.

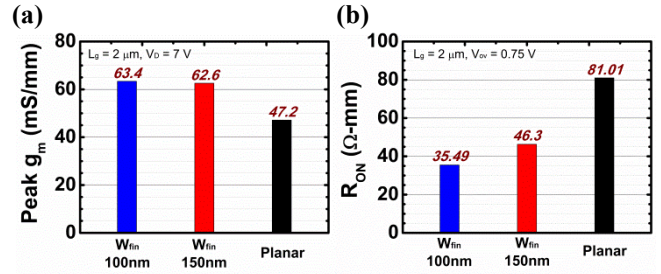


Fig. 6. Comparison of (a) peak g_m and (b) R_{ON} with different W_{fin} .

contrary to the conventional Si-based FinFET that thinner fin has larger R_{ON} due to the larger scattering. This is caused by the higher thermal resistance in the larger channel width [6].

4. Conclusions

In this paper, we demonstrate the AlGaIn/GaN Fin-HEMT with the Schottky gate contact. This Schottky contact is beneficial to pinch off the channel earlier from the sidewall. The device with minimum W_{fin} of 100 nm exhibits V_{TH} of -0.7 V which has 3.05 V shift from the planar one. The E-mode operation can be achieved with further scaling the W_{fin} down to 35 nm. The device with thinner W_{fin} also shows better ON-state performance which is caused by the lower thermal resistance.

Acknowledgements

The author would like to thank financial support provided by the Ministry of Science and Technology, R. O. C under the grant No. MOST 106-2923-E-002-006-MY3 and Industrial Technology Research Institute, R. O. C.

References

- [1] U. K. Mishra and T. E. Kazior, *Proc. IEEE*, vol. 96, no. 2, pp. 287–305, Feb. 2008.
- [2] J. W. Chung, W. E. Hoke, E. M. Chumbes, *et al.*, *IEEE Electron Device Lett.*, vol. 31, no. 3, pp. 195–197, Mar. 2010.
- [3] J. W. Chung *et al.*, *IEEE Electron Device Lett.*, vol. 30, no. 9, pp. 904–906, Sep. 2009.
- [4] K. S. Im *et al.*, *IEEE Trans. Electr. Devices*, vol. 60, no. 10, pp. 3012–3018, Oct. 2013.
- [5] B. Lu *et al.*, *IEEE Electron Device Lett.*, vol. 33, no. 3, pp. 360–362, Mar. 2012.
- [6] L.-C. Chang *et al.*, *Proc. of SPIE Vol.* Vol. 10104. 2017.